Non-Gaussian energy landscape of a simple model for strong network-forming liquids: Accurate evaluation of the configurational entropy

A. J. Moreno[a)]
Dipartimento di Fisica, Università degli Studi di Roma 'La Sapienza,' Piazzale Aldo Moro 2, I-00185 Roma, Italy; CNR-INFM-SMC, Università degli Studi di Roma 'La Sapienza,' Piazzale Aldo Moro 2, I-00185 Roma, Italy; and Donostia International Physics Center, Paseo Manuel de Lardizabal 4, E-20018 San Sebastián, Spain

I. Saika-Voivod
Dipartimento di Fisica, Università degli Studi di Roma 'La Sapienza,' Piazzale Aldo Moro 2, I-00185 Roma, Italy and Deparment of Chemistry, University of Saskatchewan, 110 Science Place, Saskatoon, Saskatchewan S7N 5C9, Canada

E. Zaccarelli
Dipartimento di Fisica, Università degli Studi di Roma 'La Sapienza,' Piazzale Aldo Moro 2, I-00185 Roma, Italy; CNR-INFM-SOFT, Università degli Studi di Roma 'La Sapienza,' Piazzale Aldo Moro 2, I-00185 Roma, Italy; and ISC-CNR, Via dei Taurini 19, I-00185 Roma, Italy

E. La Nave
Dipartimento di Fisica, Università degli Studi di Roma 'La Sapienza,' Piazzale Aldo Moro 2, I-00185 Roma, Italy; CNR-INFM-SOFT, Università degli Studi di Roma 'La Sapienza,' Piazzale Aldo Moro 2, I-00185 Roma, Italy; and ISC-CNR, Via dei Taurini 19, I-00185 Roma, Italy

S. V. Buldyrev
Department of Physics, Yeshiva University, New York, New York 10033

P. Tartaglia
Dipartimento di Fisica, Università degli Studi di Roma 'La Sapienza,' Piazzale Aldo Moro 2, I-00185 Roma, Italy and CNR-INFM-SMC, Università degli Studi di Roma 'La Sapienza,' Piazzale Aldo Moro 2, I-00185 Roma, Italy

F. Sciortino
Dipartimento di Fisica, Università degli Studi di Roma 'La Sapienza,' Piazzale Aldo Moro 2, I-00185 Roma, Italy and CNR-INFM-SOFT, Università degli Studi di Roma 'La Sapienza,' Piazzale Aldo Moro 2, I-00185 Roma, Italy

(Received 4 January 2006; accepted 24 March 2006; published online 26 May 2006)

We present a numerical study of the statistical properties of the potential energy landscape of a simple model for strong network-forming liquids. The model is a system of spherical particles interacting through a square-well potential, with an additional constraint that limits the maximum number of bonds $N_{\max}$ per particle. Extensive simulations have been carried out as a function of temperature, packing fraction, and $N_{\max}$. The dynamics of this model are characterized by Arrhenius temperature dependence of the transport coefficients and by nearly exponential relaxation of dynamic correlators, i.e., features defining strong glass-forming liquids. This model has two important features: (i) Landscape basins can be associated with bonding patterns. (ii) The configurational volume of the basin can be evaluated in a formally exact way, and numerically with an arbitrary precision. These features allow us to evaluate the number of different topologies the bonding pattern can adopt. We find that the number of fully bonded configurations, i.e., configurations in which all particles are bonded to $N_{\max}$ neighbors, is extensive, suggesting that the configurational entropy of the low temperature fluid is finite. We also evaluate the energy dependence of the configurational entropy close to the fully bonded state and show that it follows a logarithmic functional form, different from the quadratic dependence characterizing fragile liquids. We suggest that the presence of a discrete energy scale, provided by the particle bonds, and the intrinsic degeneracy of fully bonded disordered networks differentiates strong from fragile behavior. © *2006 American Institute of Physics*. [DOI: 10.1063/1.2196879]

I. INTRODUCTION

When a liquid is fastly supercooled into a metastable state under the melting point, its structural relaxation time τ increases over 13 orders of magnitude with the decreasing temperature T. Below some given temperature, equilibration is not possible within laboratory time scales, and the system becomes a glass.[1,2] The glass transition temperature T_g is operationally defined as that where $\tau=100$ s, or the viscosity $\eta=10^{13}$ P.

[a)]Electronic mail: wabmosea@sq.ehu.es

Angell has introduced a useful classification scheme[3] for glass-forming liquids. According to the definition of kinetic fragility, a liquid is classified as "strong" or "fragile" depending on how fast its relaxation time increases when approaching T_g. Liquids that show a weak dependence, well described by an Arrhenius law $\tau \propto \exp(A/T)$, where A is a temperature independent quantity, are classified as strong. Strong liquids form open network structures that do not undergo strong structural changes when decreasing temperature. In general, polymeric or low molecular weight organic liquids are fragile liquids. In these systems, where interactions show a less directional character than in strong liquids, dynamics are very sensitive to temperature changes, and relaxation times show strong deviations from Arrhenius behavior [4,5] Several empirical functions have been proposed for the T dependence of τ in fragile liquids—the Vogel-Tammann-Fulcher (VTF) law, $\tau \propto \exp[A/(T-T_0)]$—having gained more acceptance.[6] In this equation T_0 is the VTF temperature.

Kauzmann noted[7] that when extrapolating to low temperatures the experimental T dependence of the configurational entropy S_{conf}, the latter became zero at a certain temperature T_K ("Kauzmann temperature") somewhere below T_g. Experiments[1,8,9] often provide the result $T_K \approx T_0$. Given the Arrhenius character of strong liquids, this comparison would also suggest that T_K is zero for these systems.

However, it must be stressed that the values of T_K and T_0 are the result of an *extrapolation* of experimental data, which in principle is not necessarily correct. In particular, an extrapolation below T_K would lead to an "entropy catastrophe:" a disordered liquid state with less entropy than the ordered crystal. In practice, the *equilibrium* liquid state at the putative T_K is never reached in experiments because the liquid falls *out of equilibrium* at $T_g > T_K$. The fate of the configurational entropy in an ideal situation where arbitrarily long equilibration time scales could be accessed is one of the key (and controversial) questions associated to the glass transition problem. One solution states that crystallization is unavoidable when approaching T_K in equilibrium.[7,10] It has also been proposed that S_{conf} changes its functional form below T_g, remaining always positive.[11] Another solution is that S_{conf} reaches zero at T_K and remains constant below it.[12–15]

Some insight into this latter question, in the physical origin of the fragility and, in general, in the relation between dynamic and thermodynamic properties of glass-forming liquids, can be obtained by investigating the potential energy landscape (PEL),[16–21] i.e., the topology of the potential energy of the liquid $U=U(\mathbf{r}^N)$. According to the inherent structure (IS) formalism introduced by Stillinger and Weber,[17] the PEL is partitioned into basins of attraction around the local minima of U. These minima are commonly known as the "inherent structures." The free energy is obtained as a sum of a "configurational" contribution, resulting from the distribution and multiplicity of the different IS's, and another "vibrational" contribution, resulting from the configurational volume available within the basin around each individual IS. The introduction of the IS formulation has motivated a great theoretical and computational effort in order to understand the connection between the statistical properties of the PEL and the dynamic behavior of supercooled liquids,[22–46] and nowadays it has become a key methodology in the field of the glass transition.

From a series of numerical investigations in models of fragile liquids, it is well established that for such systems the distribution of inherent structures is well described by a Gaussian function, at least in the energy range that can be probed within the equilibration times permitted by computational resources.[23,29,46] It can be formally proved[13,47] that for a Gaussian landscape the energy of the average visited IS depends linearly on T^{-1}, a result that has been verified in several numerical studies of fragile liquids.[24,29,34–36] Recent studies of the atomistic BKS model for silica,[31,43] the archetype of a strong liquid behavior, have shown instead that deviations from Gaussianity take place in the low energy range of the landscape, and indeed, at low temperatures, the average inherent structure progressively deviates from linearity in T^{-1}. The existence of a lower energy cutoff and a discrete energy scale, as it would be expected for a connected network of bonds, has been proposed as the origin of such deviations from Gaussianity.[43] These investigations also suggest that S_{conf} cannot be extrapolated to zero at a finite T, and as a consequence, strong liquids would not show a finite T_K. However, long equilibration times prevent the determination of the lowest energy state and its degeneracy, and therefore an unambiguous confirmation of this result.

Recently, we have proposed a minimal model which we believe capture the essence of the prototype strong liquid behavior. In this model,[48] particles interact via a spherical square-well potential with an additional constraint on the maximum number of bonded neighbors, N_{max}, per particle. The lowest energy state is the fully bonded network, and its energy is thus unambiguously known. Within the equilibration times permitted by present day numerical resources, configurations with more than 98% of the bonds formed can be properly thermalized. As a result, no extrapolations are required to determine the low T behavior. This model is particularly indicated for studying the statistical properties of the landscape. In analogy with the Stillinger-Weber formalism, we propose to partition the configuration space in basins which, for the present case, can be associated with bonding patterns. A precise definition of the volume in the configuration space associated to each bonding pattern can be provided, since a basin is characterized by a flat surface with an energy proportional to the number of bonds. Crossing between different basins can be associated to bond-breaking or bond-forming events. In contrast to other systems previously investigated, the vibrational contribution of the PEL can be expressed in a formally exact way. No approximation for the shape of the basins is requested. As we discuss in the following, the precision of the evaluation of the basin volume, only limited by the numerical accuracy of statistical averages, allows us to evaluate, with the same precision, the configurational entropy.

In this article we report the study of the statistical properties of the N_{max} model for the cases $N_{\mathrm{max}}=3$, 4, and 5 and for a large range of packing fractions ϕ, extending the results limited to a fixed ϕ and $N_{\mathrm{max}}=4$ previously reported in a short communication.[48] The range of ϕ values here investi-

gated are (0.2–0.35) for $N_{max}=3$, (0.3–0.5) for $N_{max}=4$, and 0.35 for $N_{max}=5$. The article is organized as follows. In Sec. II we introduce the model and provide computational details. In Sec. III we briefly summarize the IS formalism and apply it to the present model. Dynamic and energy landscape features are shown and discussed in Sec. IV. Conclusions are given in Sec. V.

II. MODEL AND EVENT-DRIVEN MOLECULAR DYNAMICS

The model we investigate is similar in spirit to one previously introduced by Speedy and Debenedetti.[49] In the present model, particles interact through a spherical square-well potential with a constraint on the maximum number of bonds each particle can form with neighboring ones. Namely, the interaction between any two particles i and j, each having less than N_{max} bonds to other particles, is given by a spherical square-well potential of width Δ and depth u_0:

$$V_{ij}(r)=\begin{cases}\infty, & r<\sigma\\ -u_0, & \sigma<r<\sigma+\Delta\\ 0, & r>\sigma+\Delta,\end{cases} \tag{1}$$

with r is the distance between i and j. When $\sigma<r<\sigma+\Delta$, particles i and j form a bond, unless at least one of them is already bonded to other N_{max} particles. If this is the case $V_{ij}(r)$ is simply a hard-sphere (HS) interaction:

$$V_{ij}(r)=\begin{cases}\infty, & r<\sigma\\ 0, & r>\sigma.\end{cases} \tag{2}$$

In the original model introduced by Speedy and Debenedetti[49] an angular constraint was imposed by avoiding three particle bonding loops. In an effort to grasp the basic structural ingredients producing strong liquid behavior, we have not implemented this additional constraint. The potential given by Eqs. (1) and (2), despite its apparent simplicity, is not pairwise additive, since at any instant the interaction between two given particles does not only depend on r but also on the number of particles bonded to them (if $\sigma<r<\sigma+\Delta$). Hence, to propagate the system not only the coordinates and velocities are requested but also the list of bonded interactions.

We also note that the model is not deterministic. Consider a configuration in which particle i is surrounded by more than N_{max} other particles within a distance of $\sigma<r<\sigma+\Delta$. Of course, only N_{max} of these neighbors are bonded to i, i.e., feel the square-well interaction. If one of the bonded neighbors moves out of the square-well interaction range (i.e., to a distance of $r>\sigma+\Delta$), a bond-breaking process occurs. According to Eq. (1), a new bond can be formed with one of the other nonbonded particles whose position is in the range of $\sigma<r<\sigma+\Delta$. If several candidates are available—where a candidate is defined as a particle whose distance from i is in the range of $\sigma<r<\sigma+\Delta$ *and* which is engaged in less than N_{max} bonds to other distinct particles—then one of them is randomly selected to form the new bond with the particle i. Of course, in each bond-breaking or bond-formation process the velocities of the two involved particles are changed to conserve energy and momentum (see also below).

Despite these complications, the model given by Eqs. (1) and (2) can be considered as among the simplest ones for simulating clustering and network formation in fluids.[50,51] It does not require three-body angular forces or nonspherical interactions. The penalty for retaining spherical symmetry is the complete absence of geometrical constraints between the bonds.

The maximum number of bonds per particle is controlled by tuning N_{max}. For a system of N particles, the lowest energy state, corresponding to the fully bonded network, has an energy $E_{fb}=-NN_{max}u_0/2$. If N_{bb} is the number of broken bonds for a given configuration of the network, the energy of that configuration is given by $E=E_{fb}+N_{bb}u_0$.

The model parameters have been set to $\Delta/(\sigma+\Delta)=0.03$, $u_0=1$, and $\sigma=1$. In the following, entropy S will be measured in units of k_B. Setting $k_B=1$, potential energy E and temperature T are measured in units of u_0. Distances are measured in units of σ. Diffusion constants and viscosities are respectively measured in units of $\sigma(u_0/m)^{1/2}$ and $(mu_0)^{1/2}\sigma^{-2}$. We have simulated a system of $N=10\,000$ particles of equal masses $m=1$, implementing periodic boundary conditions in a cubic cell of length L_{box}. We have evaluated the PEL properties for several values of N_{max}, in a wide range of T, and packing fraction $\phi=\pi N/6L_{box}^3$. The system does not exhibit phase separation for the state points here investigated.[52–54]

Dynamic properties are calculated by molecular dynamics simulations. We use a standard event-driven algorithm[55] for particles interacting via discontinuous step potentials. The algorithm calculates, from the particle positions and velocities at a given instant t_0, the instants t_{coll} and positions for all possible collisions between distinct pairs and selects the one which occurs at the smallest t_{coll}. Then the system is propagated for a time $t_{coll}-t_0$ until the collision occurs. Between collisions, particles move along straight lines with constant velocities. Collisions can take place at a relative distance of $r=\sigma$ (in which case velocities of colliding particles are reversed according to hard-sphere rules) and, only for bonded interactions, at a distance of $\sigma+\Delta$ (in which case velocities are changed in such a way to conserve energy and momentum). Starting configurations are selected from previously generated hard-sphere configurations with a hard-sphere radius $\sigma+\Delta$. In this way, we start always from a configuration where no bonds are present. After thermalization at high T using the potential defined in Eqs. (1) and (2), the system is quenched and equilibrated at the requested temperature. Equilibration is achieved when energy and pressure show no drift and when particles have diffused, in average, several diameters. We also confirm that dynamic correlators and mean squared displacements show no aging, i.e., no time shift when being evaluated starting from different time origins. Once the system is equilibrated, a constant energy run is performed for the production of configurations, from which diffusivities and dynamic correlators are computed. Statistical averages are performed over typically 50–100 independent samples. Standard Monte Carlo (MC) simulations

are carried out for the calculation of the vibrational contribution of the PEL (see Sec. III), using previously equilibrated configurations.

III. INHERENT STRUCTURE FORMALISM

If $U=U(\mathbf{r}^N)$ is the potential energy of a system of N identical particles of mass m, the partition function is given by the product $Z=Z^{\mathrm{ig}}Z^{\mathrm{ex}}$, where Z^{ig} is the purely kinetic ideal gas contribution, and Z^{ex} is the excess contribution resulting from the interaction potential. The ideal gas contribution to the free energy $F^{\mathrm{ig}}=-k_BT\ln Z^{\mathrm{ig}}$ is given by

$$\beta F^{\mathrm{ig}}/N=\ln(N/V)+3\ln\Lambda-1, \tag{3}$$

where V is the system volume, $\beta=(k_{\mathrm{B}}T)^{-1}$, and $\Lambda=h(2\pi mk_BT)^{-1/2}$ is the de Broglie wavelength, where h is the Planck constant. The excess contribution to the partition function is

$$Z^{\mathrm{ex}}=\int d\mathbf{r}^N\exp[-\beta U(\mathbf{r}^N)]. \tag{4}$$

The IS formalism introduced by Stillinger and Weber[17] provides a method for calculating Z^{ex}. According to Stillinger and Weber the configuration space is partitioned into basins of attraction of the local minima of the PEL, the so-called inherent structures. If $\Omega(E_{\mathrm{IS}})$ is the degeneracy of a given IS, i.e., the number of local minima of $U(\mathbf{r}^N)$ with potential energy E_{IS}, the configurational entropy is defined as $S_{\mathrm{conf}}(E_{\mathrm{IS}})=k_B\ln[\Omega(E_{\mathrm{IS}})]$. To properly evaluate Z^{ex}, besides the information of the number of distinct IS's, it is necessary to evaluate the partition function $Z^{\mathrm{ex}}_{\mathrm{vib}}(T,E_{\mathrm{IS}})$ constrained in the volume of each of these basins. The quantity $Z^{\mathrm{ex}}_{\mathrm{vib}}(T,E_{\mathrm{IS}})$ provides a measure of the configurational volume explored at temperature T by the system constrained in the basin of depth E_{IS}. Averaging over all basins with the same depth E_{IS} one obtains[17]

$$Z^{\mathrm{ex}}_{\mathrm{vib}}(T,E_{\mathrm{IS}})=\frac{1}{\Omega(E_{\mathrm{IS}})}\sum_{\mathrm{basins}(E_{\mathrm{IS}})}\int_{\mathrm{basin}}d\mathbf{r}^Ne^{-\beta(U-E_{\mathrm{IS}})}, \tag{5}$$

where the notation "basins (E_{IS})" recalls that the sum is performed over all the basins whose potential energy minimum is E_{IS}, and each integral runs over the configurational volume associated to the corresponding basin. It is convenient to express $Z^{\mathrm{ex}}_{\mathrm{vib}}(T,E_{\mathrm{IS}})$ as

$$Z^{\mathrm{ex}}_{\mathrm{vib}}(T,E_{\mathrm{IS}})=e^{-\beta f^{\mathrm{ex}}_{\mathrm{vib}}(T,E_{\mathrm{IS}})} \tag{6}$$

to stress that the "free energy" $f^{\mathrm{ex}}_{\mathrm{vib}}(T,E_{\mathrm{IS}})$, commonly referred as the vibrational PEL contribution, accounts for the vibrational properties of the system constrained in a typical basin of depth E_{IS}.

Within the above framework, the excess partition function is given by

$$Z^{\mathrm{ex}}=\sum_{\mathrm{IS}}e^{-\beta[E_{\mathrm{IS}}-TS_{\mathrm{conf}}(E_{\mathrm{IS}})+f^{\mathrm{ex}}_{\mathrm{vib}}(T,E_{\mathrm{IS}})]}. \tag{7}$$

In the thermodynamic limit the excess free energy $F^{\mathrm{ex}}=-k_BT\ln Z^{\mathrm{ex}}$ can be evaluated as

$$F^{\mathrm{ex}}(T)=E(T)-TS_{\mathrm{conf}}(E(T))+f^{\mathrm{ex}}_{\mathrm{vib}}(T,E(T)), \tag{8}$$

where $E(T)$ is the average IS potential energy at temperature T. Therefore, the excess free energy is the sum of three contributions. The fist term in Eq. (8) accounts for the average value of the visited local minima of the potential energy. The second term is related to the degeneracy of the typical minimum. The third term accounts for the configurational volume of the typical visited basin.

The IS formalism has been applied in the past to several numerical studies of models of liquids. Indeed, simulations offer a convenient way to evaluate $F^{\mathrm{ex}}(T)$, $E(T)$, and $f^{\mathrm{ex}}_{\mathrm{vib}}(T,E(T))$ and to derive, by appropriate substractions, the configurational entropy. The only approximation performed in these studies refers to the vibrational free energy, which is usually calculated under the harmonic approximation—by solving the eigenfrequencies of the Hessian matrix evaluated at the IS—or, in the best cases, including anharmonic contributions under the strong assumption[56] that these corrections do not depend on the value of E_{IS}.

In the case of the $N_{\max}$ model, the evaluation of the free energy in the Stillinger-Weber formalism is straightforward. The partition function can be formally written as a sum over all distinct bonding patterns—i.e., over all configurations which cannot be transformed by deformation to each other without breaking/forming bonds—in a way that is formally analogous to the IS approach once one identifies a bonding pattern with an IS basin. Different from the standard IS approach, the present specific stepwise potential does not require a minimization procedure to locate the local minimum. Each bonding pattern can be associated to a basin characterized by a flat surface with an energy proportional to the number of bonds. Crossing between different basins requires bond-breaking or bond-forming events. While in the IS formalism the partition function is associated to local minima, in the $N_{\max}$ model Z^{ex} is evaluated by expanding around all distinct bonding patterns. The flat surface of the basin and the clear-cut basin boundaries make it possible to evaluate the vibrational contribution of the PEL in a formally exact way, in contrast to other systems previously investigated. No approximation for the shape of the basins is requested. In the $N_{\max}$ model, the excess vibrational free energy $f^{\mathrm{ex}}_{\mathrm{vib}}$ is purely entropic.

To calculate $f^{\mathrm{ex}}_{\mathrm{vib}}$ we make use of the Perturbed Hamiltonian approach introduced by Frenkel and Ladd[57,58] which provides an exact analytical formulation for the excess free energy of a given system by integration from a reference Einstein crystal. In brief, to calculate the free energy of a system defined by a Hamiltonian H, one can add a harmonic perturbation, $H_\lambda(\mathbf{r}^N;\lambda_{\max})=\lambda_{\max}\Sigma_{i=1}^N(\mathbf{r}_i-\mathbf{r}_i^0)^2$, around a disordered configuration $\mathbf{r}^{N_0}=(\mathbf{r}_1^0,\ldots,\mathbf{r}_N^0)$. It can be demonstrated that the excess free energies of the perturbed, $F^{\mathrm{ex}}(T;\lambda_{\max})$, and unperturbed, $F^{\mathrm{ex}}(T;\lambda=0)$, systems are related as[57–59]

$$F^{\mathrm{ex}}(T;\lambda=0)=F^{\mathrm{ex}}(T;\lambda_{\max})-\int_{-\infty}^{\ln[\lambda_{\max}]}\lambda\left\langle\sum_{i=1}^N(\mathbf{r}_i-\mathbf{r}_i^0)^2\right\rangle_\lambda d\ln[\lambda]. \tag{9}$$

Brackets denote ensemble average for fixed λ. Due to the

presence of the harmonic perturbation, particles in the perturbed system $(H+H_\lambda)$ remain constrained around $\mathbf{r}^{N_0}$. As a consequence, $\langle\Sigma_{i=1}^{N}(\mathbf{r}_i-\mathbf{r}_i^0)^2\rangle_\lambda$ is finite. For a sufficiently large value of λ_{max} (so that H is negligible as compared to H_λ), the perturbed system behaves like an Einstein crystal, i.e., like a system of $3N$ independent harmonic oscillators with elastic constant λ_{max}. The excess free energy for the latter system is given by

$$\beta F^{ex}(\lambda_{max})/N = \beta E/N - \frac{3}{2}\ln\left(\frac{\pi k_B T}{\lambda_{max}}\right) + 1 - \ln(N/V). \tag{10}$$

In this expression E is the energy of the system in $\mathbf{r}^{N_0}$. If the condition $\lambda_{max}\langle\Sigma_{i=1}^{N}(\mathbf{r}_i-\mathbf{r}_i^0)^2\rangle_{\lambda_{max}}=3Nk_BT/2$ is fulfilled, the harmonic limit is recovered and will be also valid for $\lambda'_{max}>\lambda_{max}$. Hence, λ_{max} can be taken as an upper cutoff for the integration in λ, since selecting a larger value λ'_{max} leads to a trivial cancelation in Eqs. (9) and (10).

Next we discuss how the perturbed Hamiltonian approach can be used for evaluating the excess vibrational free energy f_{vib}^{ex} of a typical bonding pattern in the N_{max} model. We start from an arbitrary equilibrium configuration $\mathbf{r}^{N_0}$ at T and with its associated bonding pattern. We then calculate, via MC, the quantity $\langle\Sigma_{i=1}^{N}(\mathbf{r}_i-\mathbf{r}_i^0)^2\rangle_\lambda$, imposing the constraint that bonds can neither break nor reform. In the limit $\lambda\to 0$ the system samples the volume in configuration space associated to the selected bonding pattern. Hence, we can identify $f_{vib}^{ex}(T,E(T))$ with $F^{ex}(T;\lambda=0)$. By retaining the constraint on the bonding pattern, we simulate the perturbed system for several values of λ to properly evaluate the integrand of Eq. (9) and estimate the value of $f_{vib}^{ex}(T,E(T))$. To improve statistics, an average over several starting configurations $\mathbf{r}^{N_0}$ is performed.

Within the above framework, the corresponding expression for the excess vibrational entropy S_{vib}^{ex} is

$$\frac{S_{vib}^{ex}}{Nk_B} = \frac{3}{2}\ln\left(\frac{\pi k_B T}{\lambda_{max}}\right) - 1 + \ln\left(\frac{N}{V}\right) + \beta\int_{-\infty}^{\ln[\lambda_{max}]}\lambda\left\langle\sum_{i=1}^{N}(\mathbf{r}_i-\mathbf{r}_i^0)^2\right\rangle_\lambda d\ln[\lambda]. \tag{11}$$

We stress that Eq. (11) is an exact relation for S_{vib}^{ex} for the present N_{max} model. Hence, the precision in the evaluation of this quantity does not depend on any approximation, but only on the numerical accuracy of the MC calculation and the statistical average.

The total excess entropy $S_{tot}^{ex}(T)$ can also be calculated with an arbitrary precision by a thermodynamic integration from a reference state at $T=T_{ref}$, where S_{tot}^{ex} is already known. One possible choice is to select as reference point the ideal gas and integrate along a path which does not cross any phase boundary or, in the present case, to integrate from very high temperatures. Indeed, at sufficiently high T_{ref}, the model is equivalent to a hard-sphere system, whose free energy is well known. An accurate estimate of the hard-sphere excess entropy is provided by the Carnahan-Starling formula:[60]

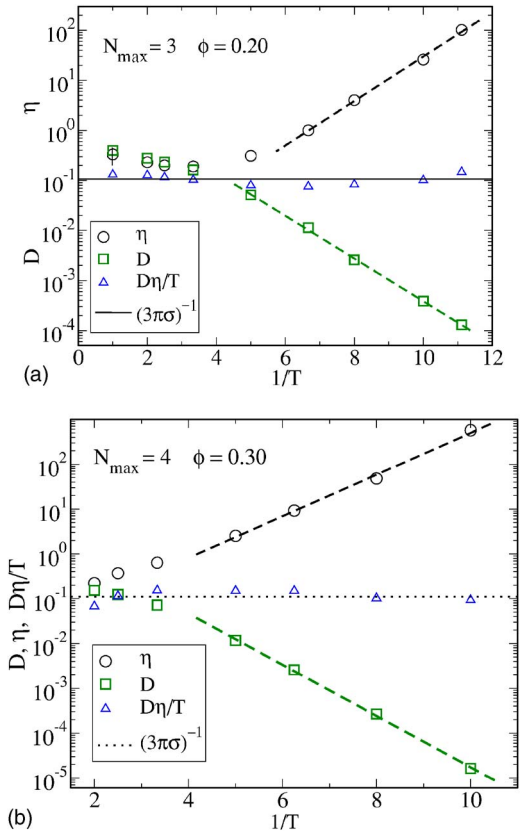

FIG. 1. T dependence of the diffusivity D, the viscosity η, and the product $D\eta/T$ for the cases $N_{max}=3$, $\phi=0.20$ (a), and $N_{max}=4$, $\phi=0.30$ (b). Dotted lines correspond to the expected value $(3\pi\sigma)^{-1}$ from the Stokes-Einstein relation. Dashed lines are fits to Arrhenius laws. An error bar is included for the viscosity at high T.

$$\frac{S_{HS}^{ex}}{Nk_B} = \frac{\phi(3\phi-4)}{(1-\phi)^2}. \tag{12}$$

The excess entropy at finite T can then be obtained by integrating along a constant volume V path as

$$S_{tot}^{ex}(T) = S_{HS}^{ex} + \int_{T_{ref}}^{T}\left(\frac{\partial E}{\partial T}\right)_V\frac{dT}{T}. \tag{13}$$

From the two accurate evaluations of S_{tot}^{ex} [Eq. (13)] and S_{vib}^{ex} [Eq. (11)] an accurate estimate of the configurational entropy S_{conf} can be obtained as $S_{conf}=S_{tot}^{ex}-S_{vib}^{ex}$. The resulting S_{conf} can be related to T or, parametrically, to $E(T)$ (i.e., to the number of bonds). In the rest of the article, all the thermodynamic functions Ψ will be expressed as "quantities per particle," but for simplicity of notation we will drop the factor $1/N$. Hence, in the following Ψ will be understood as Ψ/N.

IV. RESULTS AND DISCUSSION

A. Dynamics

In this section we show that the dynamics in the N_{max} model meet the criteria defining strong liquids. The key feature is the Arrhenius behavior of the transport coefficients. Figure 1 shows the T dependence of the diffusivity D and the viscosity η for different values of N_{max} and ϕ. The diffusiv-

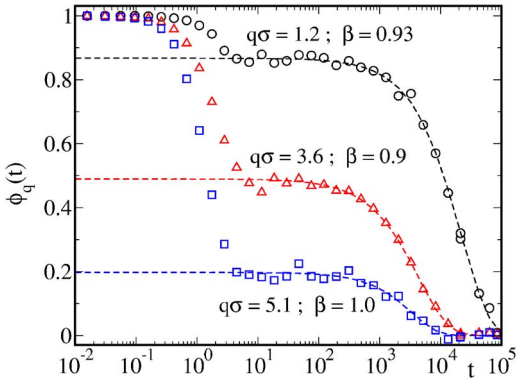

FIG. 2. Symbols: Coherent intermediate scattering function for $N_{max}=4$, $\phi=0.30$, and $T=0.1$ for different values of the wave vector q. Dashed lines are KWW fits. The stretching exponents β are indicated for the corresponding q's.

ity is calculated as the long time limit of $\langle\Sigma_{i=1}^{N}[\mathbf{r}_i(t)-\mathbf{r}_i(0)]^2\rangle/6Nt$. The viscosity η is determined as

$$\eta=\frac{1}{2Vk_BT}\lim_{t\to\infty}\frac{d}{dt}\langle[A(t)-A(0)]^2\rangle, \tag{14}$$

where $A(t)=m\Sigma_{i=1}^{N}\dot{r}_i^{\alpha}r_i^{\beta}$, as explained in Ref. 61. Greek symbols denote the x, y, and z coordinates of the position $\mathbf{r}_i$ of particle i. An average is done over all the permutations with $\alpha\neq\beta$. As shown in Fig. 1, at low temperatures both quantities display Arrhenius behavior. The activation energies for D and η are approximately u_0, suggesting that all bonds break and reform essentially in an independent way. This is consistent with the absence of angular constraints in this model. Despite the limited simulations in time by computational resources, the fact that the Arrhenius form covers more than three orders of magnitude and the observed value of the activation energy strongly suggest that this functional form will be retained at lower T. We also find (see Fig. 1) that the Stokes-Einstein relation[62] $D\eta/T=(3\pi\sigma)^{-1}$ is fulfilled essentially at all temperatures, independently from the N_{max} value.

Long time decays of dynamic correlators in supercooled states are usually well described by the phenomenological Kohlrausch-Williams-Watts (KWW) function $\exp[-(t/\tau)^{\beta}]$, where τ is the corresponding relaxation time and β is a stretching exponent which takes values of $0<\beta<1$. The experimental evidence for a collection of chemically and structurally very different glass-forming liquids[4] shows that the smaller the fragility index (i.e., the closer the system is to a strictly strong behavior), the closer to unity the values of β are. Figure 2 shows that this is indeed the case for the N_{max} model. The long-time dependence of the normalized coherent intermediate scattering function $\phi_q(t)=\langle\rho_q(t)\rho_{-q}(0)\rangle/\langle\rho_q(0)\rho_{-q}(0)\rangle$, where $\rho_q(t)=\Sigma_{i=1}^{N}\exp[i\mathbf{q}\cdot\mathbf{r}_i(t)]$, can be well described by KWW fits, with values of $\beta>0.85$ in all the q range and for all studied ϕ. Such a behavior is observed at all T where the system shows Arrhenius behavior. As shown in Ref. 4, these β values are very different from the ones typical of fragile liquids ($\beta\sim0.5$).

Results reported in Figs. 1 and 2 provide a convincing evidence that Eqs. (1) and (2) define a simple and satisfactory minimal model for a strong glass-forming liquid.

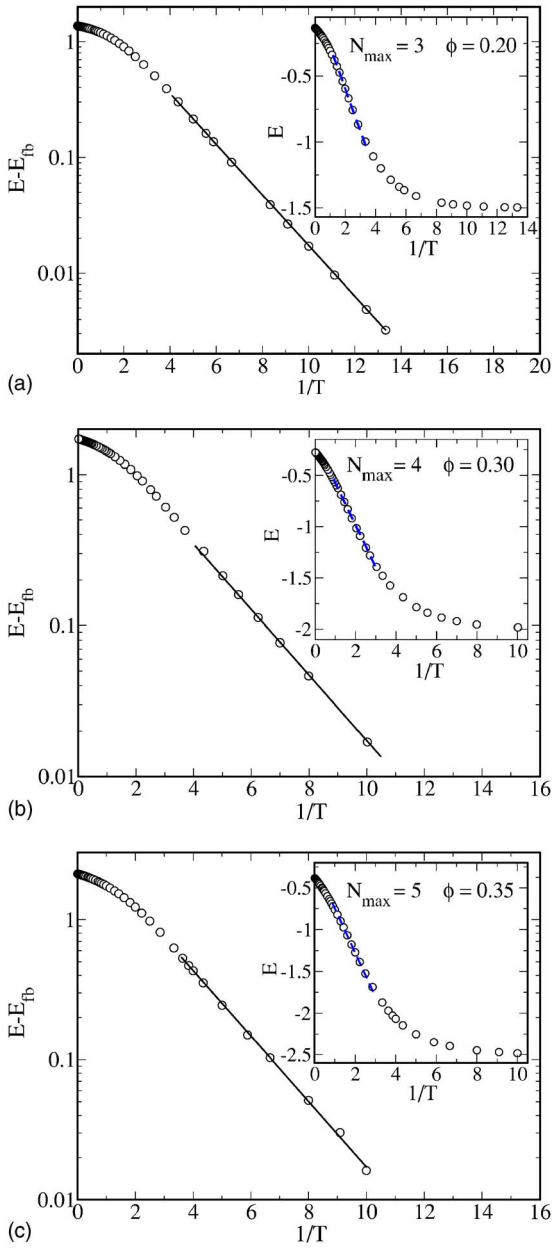

FIG. 3. T dependence of the potential energy per particle E for the cases $N_{max}=3$, $\phi=0.20$ (a), $N_{max}=4$, $\phi=0.30$ (b), and $N_{max}=5$, $\phi=0.35$ (c). Full lines at low T are fits to Arrhenius behavior with the activation energy $u_0/2$ (see text and Table I). Dashed lines at high T correspond to linear behavior in T^{-1} (see text).

B. Energy landscape

Figure 3 shows the T dependence of the potential energy (i.e., the energy of the typical bonding pattern) per particle, E. In the present model, the potential energy of each configuration coincides with the energy of the bonding pattern and can be directly associated, in the Stillinger-Weber formalism, with the IS energy. Within the times accessible by the simulations, equilibrium states can be reached for configurations characterized by a number of broken bonds smaller than 2%; i.e., the lowest energy state, E_{fb}, is approached from equilibrium simulations.

From the low T behavior of E, one sees that the approach to E_{fb} is well described by an Arrhenius law:

TABLE I. Fit parameters for the low T Arrhenius dependence of the potential energy E (see text).

$(N_{\max}, \phi)$	A_∞	A_∞^f	ϵ_f
(3, 0.20)	2.69	2.70	0.506
(3, 0.30)	1.74	1.72	0.499
(3, 0.35)	1.38	1.37	0.498
(4, 0.30)	2.59	2.73	0.508
(4, 0.35)	2.15	2.12	0.498
(4, 0.40)	1.70	1.67	0.498
(4, 0.45)	1.28	1.23	0.495
(4, 0.50)	0.900	0.884	0.498
(5, 0.35)	3.14	3.73	0.539

$$E - E_{\rm fb} = A_\infty^f \exp(-\epsilon_f/k_B T). \quad (15)$$

The activation energy ϵ_f, determined by a free fit, is close to $u_0/2$. Indeed, by forcing the Arrhenius activation energy to be exactly $u_0/2$ a satisfactory representation of the data is recovered, with one simple fitting parameter A_∞. Figure 3 shows the result of a fit to $E-E_{\rm fb}=A_\infty \exp(-u_0/2k_BT)$. The corresponding best-fitting values, with two (A_∞^f, u_0) and one (A_∞) free parameters are reported in Table I. The observed value $u_0/2$ is consistent with theoretical predictions based on the thermodynamic perturbation theory developed by Wertheim[63] to study association in simple liquids. It is not a coincidence since in Wertheim's theory bonds are also geometrically uncorrelated. Similar values are also predicted by more intuitive recent approaches.[64]

The clear low T Arrhenius dependence and the explicit value of the activation energy provide a convenient way to evaluate the T dependence of the energy for lower T. While in T it might appear as a wide extrapolation procedure, we recall that in E the *interpolation* extends only over a small (2%) range of energies between the fully bonded state ($E=E_{\rm fb}$) and the lowest equilibrated state studied in simulations. Equation (15) provides a convenient expression for the low T behavior of E and, by using Eq. (13), a way of calculating the total excess entropy down to the fully connected state.

We note in passing that at intermediate temperatures the T dependence of E is consistent with a $1/T$ law, as expected for a Gaussian distribution of energy levels. The $1/T$ law crosses to the Arrhenius dependence on cooling. This crossing has been also observed in the study of the T dependence of the IS energy in a realistic (atomistic) model for silica.[31,43]

The low T Arrhenius dependence of E [Eq. (15)] has a practical implication in the T dependence of the isochoric configurational specific heat $C_V^{\rm conf}(T)=(\partial E/\partial T)_V$. Hence, from Eq. (15), at low T we have $C_V^{\rm conf}(T)=A_\infty^f \epsilon_f k_B^{-1} T^{-2} \times \exp(-\epsilon_f/k_BT)$, which has a maximum at $T=\epsilon_f/2 \approx u_0/4$. Figure 4 shows that, indeed, numerical data for $C_V^{\rm conf}$ display a peak at $T\approx 0.25$. A peak in $C_V^{\rm conf}(T)$ has also been observed in recent simulations of atomistic models of two different network-forming liquids: silica[31] and BeF_2.[65]

We note that a strong correlation is observed between the T dependence of the diffusivity and the T dependence of the potential energy. Figure 5 shows, for $N_{\max}=4$ and several ϕ values, that on cooling, D crosses to an Arrhenius law at

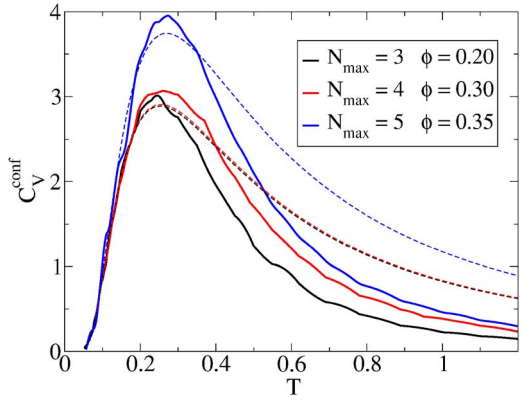

FIG. 4. Full lines: T dependence of the isochoric configurational specific heat for several values of $(N_{\max}, \phi)$. Dashed lines are an extrapolation to high T of the low T behavior $A_\infty^f \epsilon_f k_B^{-1} T^{-2} \exp(-\epsilon_f/k_BT)$ (see text).

$T\approx 0.25$. This temperature is the same at which the specific heat shows a maximum. This correlation holds at all the investigated ϕ values.

The quality of the low T Arrhenius fits for the diffusivities are worse at high ϕ. Indeed, low T data at high ϕ show some bending [Fig. 5(a)]. This result suggests that the system will become more fragile with the increasing density. This is not surprising, since the influence of the square well will be weaker at a higher packing, and the system will approach a dense hard-sphere liquid, which is a fragile system.

Next we turn to the evaluation of the statistical properties of the PEL, and more precisely the total excess entropy

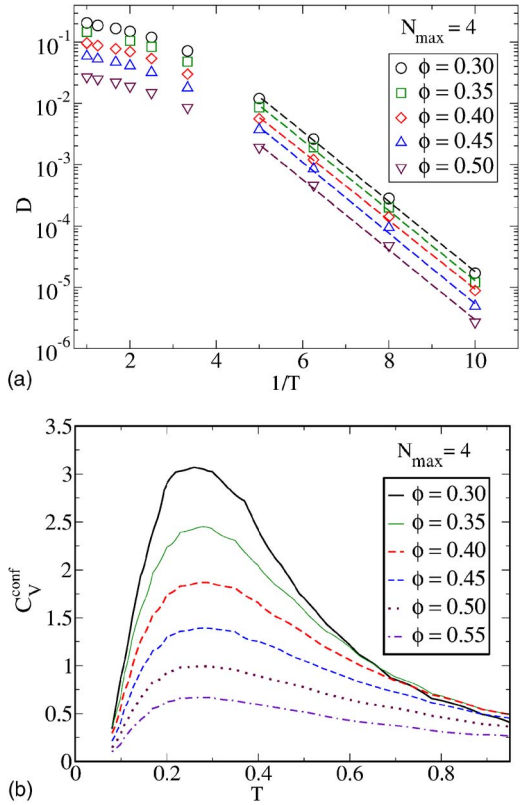

FIG. 5. T dependence of the diffusivity (a) and the isochoric configurational specific heat (b) for $N_{\max}=4$ at several values of ϕ. Dashed lines in the panel (a) are Arrhenius fits.

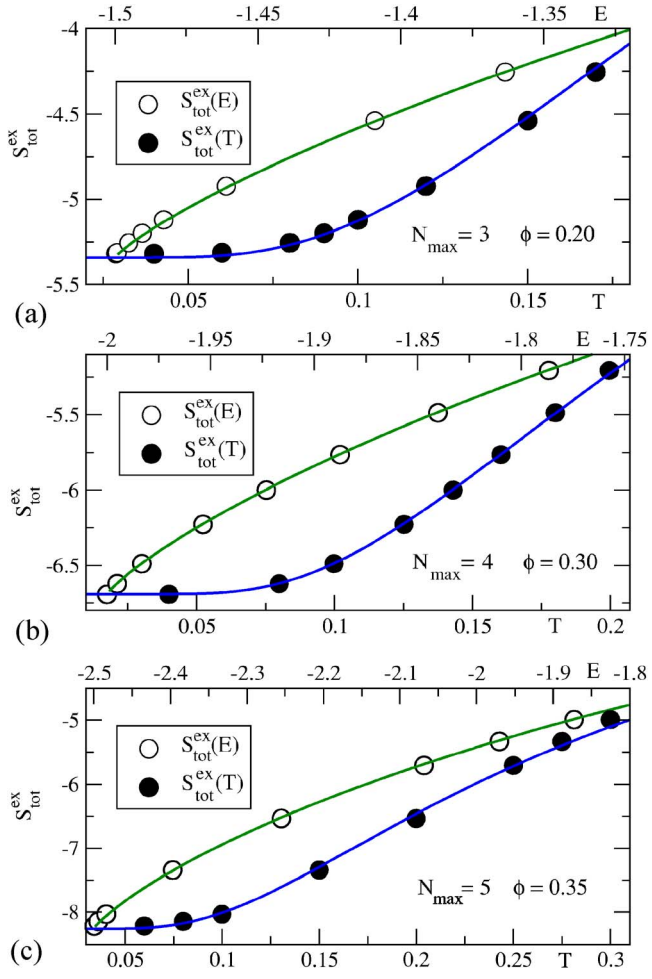

FIG. 6. E and T dependences of the total excess entropy over the ideal gas value, S^{ex}_{tot}, for the cases $N_{max}=3$, $\phi=0.20$ (a), $N_{max}=4$, $\phi=0.30$ (b), and $N_{max}=5$, $\phi=0.35$ (c). Continuous lines for $S^{ex}_{tot}(E)$ are obtained as the sum of the fit functions for $S^{ex}_{vib}(E)$ [Eq. (16)] and $S_{conf}(E)$ [Eq. (19)]. Continuous lines for $S^{ex}_{tot}(T)$ are parametrically obtained from the T dependence of E.

and its vibrational and configurational contributions. As explained in Sec. III [Eq. (13)], the total excess entropy S^{ex}_{tot} is evaluated by an isochoric integration from the hard-sphere limit at a sufficiently high T_{ref}. We use a value $T_{ref}=100$. Figure 6 shows S^{ex}_{tot} as a function of T and E, for different values of ϕ and N_{max}. Due to the presence of the interaction potential (1) and (2), S^{ex}_{tot} is negative (see also below). As expected, $S^{ex}_{tot}(T)$ decays to a constant value at low T, since the system is very close to the fully bonded state and no further structural changes are expected to occur. A glass transition temperature T_g can be operationally defined as the T at which relaxation becomes longer than the simulation time. The fact that the system is so close to its lowest energy state already above this operational T_g implies that a very small drop of the specific heat is expected at T_g, consistent with the experimental evidence in strong liquids.[5]

The evaluation of the vibrational contribution S^{ex}_{vib} [Eq. (11)] requires the calculation of the integral over the coupling constants λ. Figure 7 shows the calculated λ dependence of $\lambda\langle\Sigma_{i=1}^{N}(\mathbf{r}_i-\mathbf{r}_i^0)^2\rangle_\lambda/N$ at several T for one specific value of N_{max} and ϕ. Data for different N_{max} and ϕ display a similar behavior. At values of $\lambda<\lambda_{min}\approx 10^{-6}$ contributions

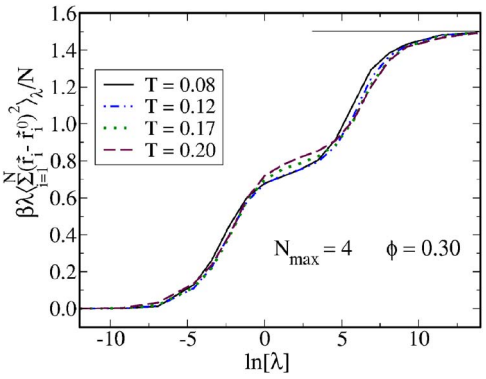

FIG. 7. λ dependence of $\beta\lambda\langle\Sigma_{i=1}^{N}(\mathbf{r}_i-\mathbf{r}_i^0)^2\rangle_\lambda/N$ for $N_{max}=4$ and $\phi=0.30$ at different temperatures. The horizontal line indicates the expected value 3/2 for the harmonic behavior.

to the integral in Eq. (11) are negligible, and λ_{min} is taken as lower cut for integration. At large λ values, $\lambda\langle\Sigma_{i=1}^{N}(\mathbf{r}_i-\mathbf{r}_i^0)^2\rangle_\lambda/N$ approaches the theoretical limit $3k_BT/2$. This value is reached at $\lambda_{max}\gtrsim 10^6$. Note that $\lambda=10^6$ corresponds to an average displacement per particle of the order of 10^{-4} for this T range. Hence the harmonic perturbation localize the particles in a well much narrower than the square-well width Δ, so that the presence of the unperturbed potential is irrelevant for this upper λ value.

Figure 8 shows the T and E dependence of S^{ex}_{vib} for the same values of ϕ and N_{max} of Fig. 6. Close to the fully connected state, S^{ex}_{vib} can be well described by a linear dependence on the energy (i.e., on the number of bonds):

$$S^{ex}_{vib}(E)=S^{ex}_{vib}(E_{fb})+\gamma_{vib}(E-E_{fb}). \tag{16}$$

Interestingly, this linear dependence on the basin depth has also been observed in previously investigated models of supercooled liquids.[19,24,29,35,36]

Finally, the configurational entropy S_{conf} is determined as $S^{ex}_{tot}-S^{ex}_{vib}$. Figure 9 shows S_{conf} for the same ϕ and N_{max} of Figs. 6 and 8. Some considerations are in order: as for the total entropy, S_{conf} approaches a constant value at low T. Interestingly enough, this constant value is significantly different from zero. The fully connected network is thus characterized by an extensive number of distinct bond configurations $\sim\exp(NS_{conf})$. These different network configurations arise from different bond topologies; i.e., disorder is associated to the presence of closed loops of different number of bonds.

To derive a functional form for the E dependence of S_{conf}, we start from the thermodynamic relation $(\partial S/\partial E)_V=1/T$, which in the present case can be written as

$$\frac{\partial(S_{conf}+S_{vib})}{\partial(E-E_{fb})}=\frac{1}{T}. \tag{17}$$

At low T, from Eq. (15) we obtain $1/T=-(1/\epsilon_f)\ln[(E-E_{fb})/A^f_\infty]$ and, making use of Eq. (16), we find

$$\frac{\partial S_{conf}}{\partial(E-E_{fb})}=-\gamma_{vib}-\frac{1}{\epsilon_f}\ln\frac{E-E_{fb}}{A^f_\infty}, \tag{18}$$

which, after integration, provides the E dependence of the configurational entropy:

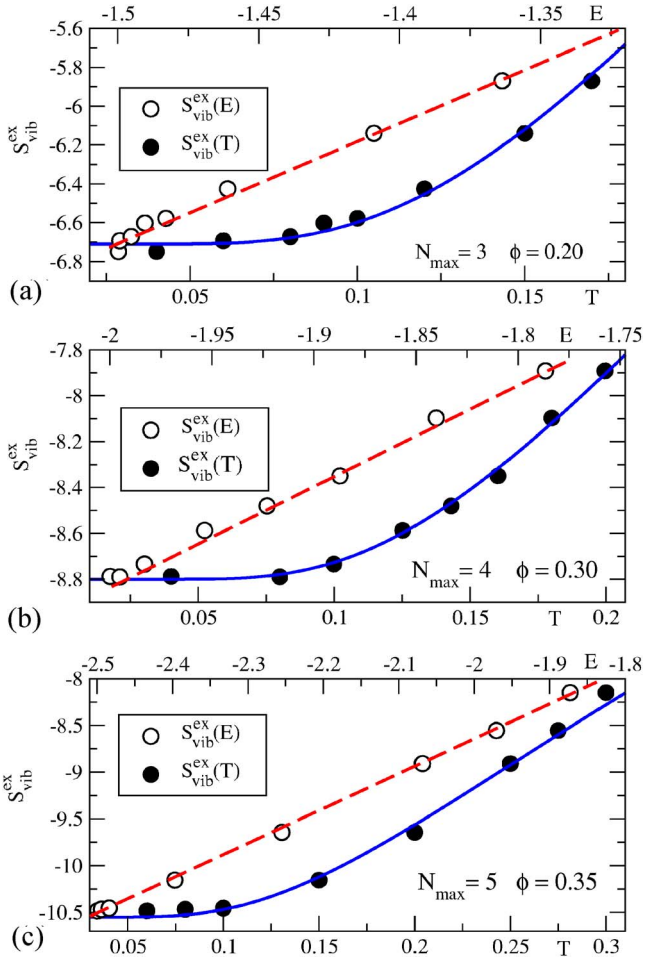

FIG. 8. Similar to Fig. 6 for the excess vibrational entropy S^{ex}_{vib}. Dashed lines for $S^{ex}_{vib}(E)$ are linear fits [Eq. (16)]. Continuous lines for $S^{ex}_{vib}(T)$ are parametrically obtained from the T dependence of E (see text).

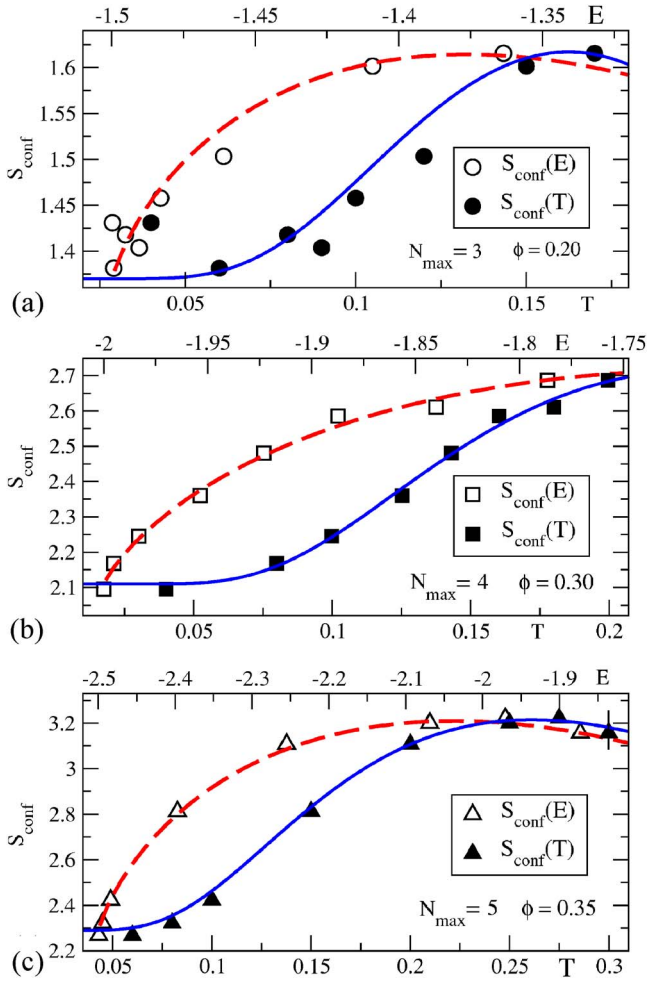

FIG. 9. Similar to Figs. 6 and 8 for the configurational entropy S_{conf}. Dashed lines for $S_{conf}(E)$ are fits to Eq. (19). Continuous lines for $S_{conf}(T)$ are parametrically obtained from the T dependence of E (see text). A typical error bar is shown in the (c) panel.

$$S_{conf}(E) = S_{conf}(E_{fb}) - \frac{E - E_{fb}}{\epsilon_f} \ln[2(E - E_{fb})] + \gamma_{conf}(E - E_{fb}), \tag{19}$$

where the constant γ_{conf} is given by

$$\gamma_{conf} = \frac{1}{\epsilon_f} - \gamma_{vib} + \frac{\ln(2A^f_\infty)}{\epsilon_f}. \tag{20}$$

As mentioned above, a satisfactory description of the low T Arrhenius dependence of E is provided by forcing a value $u_0/2$ for the activation energy ϵ_f. Hence, we can make the changes $\epsilon_f \to u_0/2$ and $A^f_\infty \to A_\infty$ in Eqs. (19) and (20). These changes allow us to obtain a simple expression of S_{conf} in terms of the number of broken bonds. Hence, since $E-E_{fb} = N_{bb}u_0$, we find

$$S_{conf}(E) = S_{conf}(E_{fb}) - 2N_{bb}\ln(2N_{bb}) + \gamma_{conf}N_{bb}. \tag{21}$$

This expression suggests that the low-E, T dependence of the configurational entropy is controlled by a combinatorial factor related to the number of broken bonds randomly distributed along the network. The derivation also shows how intimately the logarithmic dependence of the entropy is connected to the Arrhenius dependence of E at low T. The final expression for $S_{conf}(E)$ is very different from the quadratic energy dependence resulting from the Gaussian distribution of IS energies observed in models of fragile liquids.[23,29,34,35]

To provide a further and analysis-free confirmation of the crossover at low T toward combinatorial statistics of the bonding energy states, we show in Fig. 10 the T dependence of E for $N_{max}=4$ at several ϕ values. We show a representation of $E-E_{fb}$, both in linear and logarithmic scales, as a function of $1/T$. We note that for all ϕ when $E-E_{fb} \approx 0.75$ the $1/T$ law, which is expected to hold in a Gaussian landscape, breaks down. Similarly, when $E-E_{fb} \approx 0.3$ the Arrhenius law sets in. The fact that both crossovers are, at most, weakly dependent on ϕ suggests that they are esentially controlled by the bonding statistics, and that between $E-E_{fb} \approx 0.75$ and $E-E_{fb} \approx 0.3$ a crossover from Gaussian to logarithmic statistics occurs.

Figure 9 shows the E and T dependence of S_{conf} for different values of N_{max}. Equation (19) provides a good description of the data. No fit parameters are involved in comparing the numerical estimates of S_{conf} and the predictions of Eq. (19), except for the constant $S_{conf}(E_{fb})$. Note that γ_{conf} is not a fit parameter but a function [Eq. (20)] of parameters defining $E(T)$ and $S^{ex}_{vib}(E)$. Before discussing the calculated

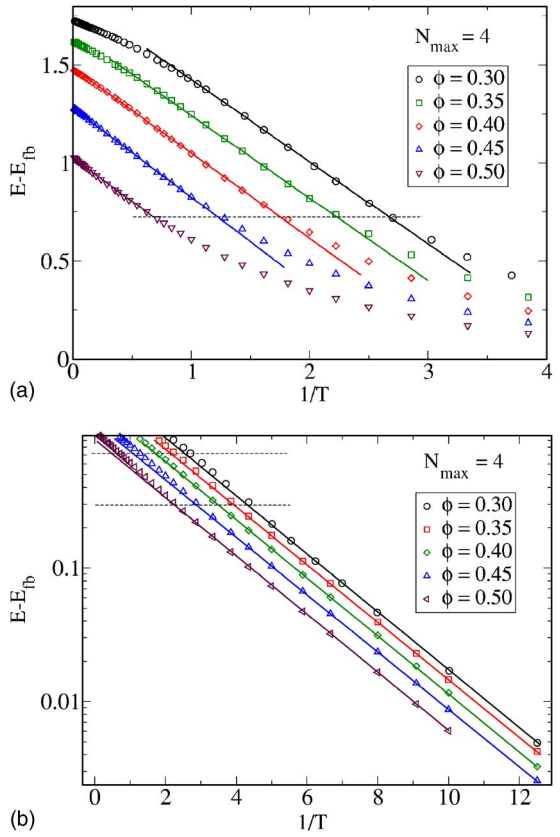

FIG. 10. T dependence of $E-E_{\mathrm{fb}}$ at different regions of the energy landscape. Top panel: Full lines correspond to linear behavior in $1/T$. The horizontal dashed line indicates the departure of such behavior. Bottom panel: Full lines correspond to Arrhenius behavior. The horizontal dashed lines indicate the limits of Arrhenius and $1/T$ behaviors.

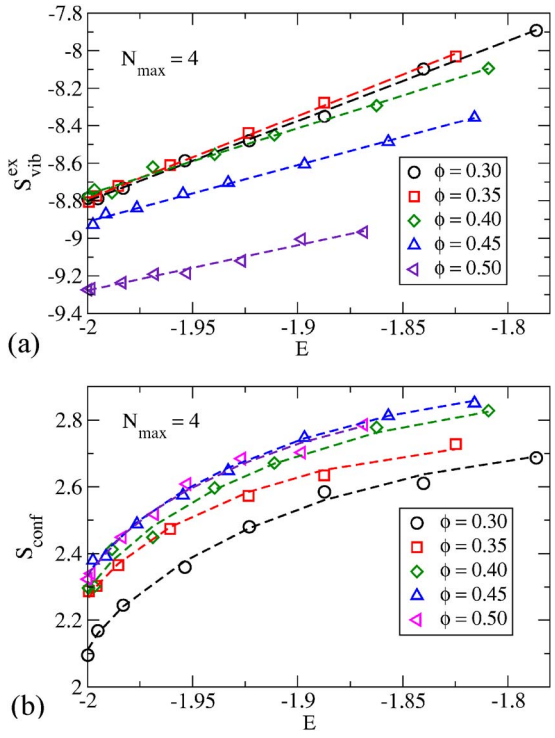

FIG. 11. E dependence of $S_{\mathrm{vib}}^{\mathrm{ex}}$ and S_{conf} for $N_{\mathrm{max}}=4$ and different values of ϕ. Dashed lines in panels (a) and (b) are, respectively, fits to Eqs. (16) and (19).

values for $S_{\mathrm{conf}}(E_{\mathrm{fb}})$, we present in Fig. 11 the E dependence of the configurational and excess vibrational entropies for $N_{\mathrm{max}}=4$ and different packing fractions ϕ. For all ϕ, the same functional forms of Eqs. (16) and (19) are recovered, respectively, for $S_{\mathrm{vib}}^{\mathrm{ex}}$ and S_{conf}. The two quantities show an opposite trend. Curves for $S_{\mathrm{conf}}(E)$ tend to collapse at high ϕ, while those for $S_{\mathrm{vib}}^{\mathrm{ex}}(E)$ tend to collapse at low ϕ. Interestingly, the configurational entropy just shifts with varying ϕ.

Table II summarizes the results of the fits of the vibrational and configurational entropies to Eqs. (16) and (19) for the studied range of control parameters. Data shown in the table help in discussing the N_{max} and ϕ dependence of the entropy of the fully bonded state. As can be observed by comparing the results for $N_{\mathrm{max}}=3$ and $N_{\mathrm{max}}=4$, increasing N_{max} produces an increase of $S_{\mathrm{conf}}(E_{\mathrm{fb}})$. This trend is much weaker between $N_{\mathrm{max}}=4$ and $N_{\mathrm{max}}=5$. A similar weak trend is observed for $N_{\mathrm{max}}=4$ by increasing ϕ. The weak increase of $S_{\mathrm{conf}}(E_{\mathrm{fb}})$ obtained by increasing ϕ suggests that when the system is compressed, neighboring particles progressively enter in the interaction range of a given one, yielding a major variety of local configurations of the bonding pattern and, consequently, more topologically distinct fully bonded networks. The trend of the excess vibrational entropy suggests that increasing ϕ leads to a decrease of the available free volume for a given bonding pattern.

A summary of the landscape analysis for all studied ϕ is shown in Fig. 12 for $N_{\mathrm{max}}=4$. The figure shows the ϕ dependence of $S_{\mathrm{tot}}^{\mathrm{ex}}$, $S_{\mathrm{vib}}^{\mathrm{ex}}$ and S_{conf} for several different low T isotherms, all in the Arrhenius region of energies. It clearly emerges that the significant reduction of $S_{\mathrm{tot}}^{\mathrm{ex}}$ on increasing ϕ arises essentially from the vibrational component. We also note that the HS relative contribution to $S_{\mathrm{tot}}^{\mathrm{ex}}$ increases on increasing ϕ. Hence, according to Eq. (12), $S_{\mathrm{HS}}^{\mathrm{ex}}(\phi=0.30)=-1.90$, while $S_{\mathrm{HS}}^{\mathrm{ex}}(\phi=0.50)=-5.0$. By comparing with data in Fig. 12, it is clear that $S_{\mathrm{tot}}^{\mathrm{ex}}$ is dominated by the square-well and hard-sphere contributions at, respectively, low and high packing fractions.

It is also interesting to observe that, within the precision of the data, S_{conf} shows a weak maximum, shifting to higher ϕ on cooling. To test whether the presence of a maximum of S_{conf} has some effect on the dynamics we also show in Fig. 12 the behavior of the diffusivity along the same isotherms.

TABLE II. Parameters defining the configurational [Eq. (19)] and excess vibrational [Eq. (16)] entropies for the studied values of N_{max} and ϕ.

(N_{max}, ϕ)	$S_{\mathrm{conf}}(E_{\mathrm{fb}})$	γ_{conf}	$S_{\mathrm{vib}}^{\mathrm{ex}}(E_{\mathrm{fb}})$	γ_{vib}
(3, 0.20)	1.37	−0.79	−6.71	6.16
(3, 0.30)	1.55	−0.336	−6.60	4.83
(3, 0.35)	1.63	−1.02	−6.70	5.05
(4, 0.30)	2.11	1.02	−8.80	4.27
(4, 0.35)	2.26	0.49	−8.79	4.43
(4, 0.40)	2.28	0.93	−8.77	3.52
(4, 0.45)	2.33	0.87	−8.91	3.01
(4, 0.50)	2.33	0.77	−9.27	2.41
(5, 0.35)	2.28	1.84	−10.55	3.83

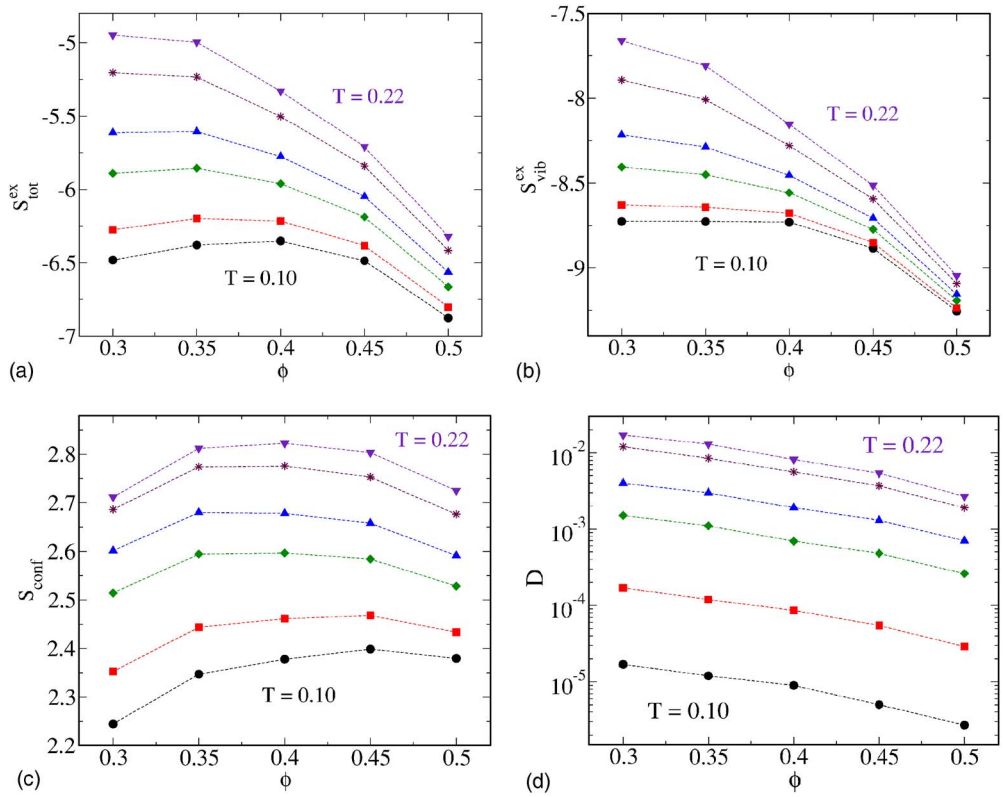

FIG. 12. ϕ dependence of $S_{\mathrm{tot}}^{\mathrm{ex}}$, $S_{\mathrm{vib}}^{\mathrm{ex}}$, S_{conf}, and D for $N_{\mathrm{max}}=4$ along isothermal curves. In all figures, from top to bottom, the isothermals are $T=0.22$, 0.20, 0.17, 0.15, 0.12, and 0.10. Dashed lines are guides for the eyes.

We note that D is monotonic in ϕ and hence that the maximum in the configurational entropy does not provoke a maximum in the diffusivity. We also note that an isochoric plot (not shown) of $\log D$ vs $[TS_{\mathrm{conf}}(T)]^{-1}$ provides a satisfactory linearization of the data, as suggested by the Adam-Gibbs theory.[66] This is not inconsistent with the observed Arrhenius dependence of D, since the T dependence of $S_{\mathrm{conf}}(T)$ is only at most 20% of $S_{\mathrm{conf}}(E_{\mathrm{fb}})$.

V. CONCLUSIONS

This article reports an explicit numerical calculation of the potential energy landscape for a simple model of strong liquids. It shows that it is possible to calculate with arbitrary precision the statistical properties of the landscape relevant to the behavior of the system at low T, when all particles are connected by bonds. The model can be seen as a zeroth order model for network-forming liquids, capturing the limited valency of the interaction and the open structure of the liquid. By construction, it misses all geometric correlations between different bonds which are present in network-forming materials. The simplicity of the model has several advantages, some of which are of fundamental importance for an exact evaluation of the landscape properties. Hence, since angular constraints between bonds are missing, it is possible to equilibrate the system to very low T, reaching configurations which are essentially fully bonded. At the lowest studied T, less than 2% of the bonds are broken on the average. Different from other studied models with fixed bonding site geometries,[67–69] the absence of geometric constraints makes it possible to reach almost fully bonded states in a wide range of densities. Moreover, the use of a square-well interaction as a bonding potential has the advantage that the energy of the fully bonded state (the lowest possible energy) is known.

The present model neglects completely interactions between particles which are not nearest neighbors. The energy of a particle is indeed fully controlled by the bonds with the nearby particles. This element of the model favors a sharp definition of the energy and a clear-cut definition of basins. On the other hand, in network-forming liquids, bonding is often of electrostatic origin and interactions are not limited to the first shell of neighbors. This produces a much wider variety of local environments and, as a consequence, a spreading of the energy levels. These residual interactions, if smaller than the bonding interactions, will only contribute to spreading the distribution of energy states without changing the landscape features (down to T of the order of the energy spreading).

The use of square-well interactions has a major advantage in relation to the possibility of precisely calculating landscape properties, since the energy of the system becomes a measure of the number of bonds. A basin in the configuration space can be identified as a bonding pattern, and a transition between different basins becomes associated to bond forming and breaking. Under these conditions, the basin boundaries are properly defined. We have shown that the method of the Perturbed Hamiltonian can be extended to the present model, providing a formally exact method to evaluate the vibrational component of the free energy. This is a relevant achievement, since the evaluation of the vibrational

entropy is the only weak point in all estimates of landscape properties in models with continuous potentials.[21,45] Indeed, when the potential is continuous, the constraint of exploring a fixed basin cannot be implemented unambiguously in the Frenkel-Ladd method due to the difficulty of detecting crossings between different basins. Such a difficulty is not present in the square-well potential, since the crossing of a basin is detected by a finite energy change.

The two relevant features observed in this study are (i) the residual value of the configurational entropy for $T \to 0$ associated to the exponentially large number of distinct fully connected bonding patterns and (ii) the logarithmic dependence of the number of bonding patterns on the number of broken bonds [Eq. (21)]. These two features are common to all investigated values of $N_{\max}$ and to all studied ϕ. A consequence of the logarithmic landscape statistics is the absence of a finite temperature at which the lowest energy state is reached.[70] Indeed from Eq. (19) it is found that $\partial S/\partial E|_{E=E_{\mathrm{fb}}}=\infty$, and hence E_{fb}, is reached only at $T=0$.

According to the picture emerging from this study, strong liquid behavior is connected to the existence of an energy scale provided by the bond energy, which is discrete and dominant as compared to the energetic contributions coming from nonbonded next-nearest neighbor interactions.[71] It is also intimately connected to the existence of a significantly degenerate lowest energy state, favoring the formation of highly bonded states which can still entropically rearrange to form different bonding patterns with the same energy. Of course, the specific value of $S_{\mathrm{conf}}(E_{\mathrm{fb}})$ in the $N_{\max}$ model provides an upper bound to the value expected in network-forming liquids,[72,73] since the absence of angular constraints significantly increases the number of geometric arrangements of the particles compatible with a fully bonded state. Recent estimates in glassy water,[74] which forms a tetrahedral disordered network, suggest a residual value of the configurational entropy of the order of $\approx 0.3k_B$. Hence the localization of the bonding sites at specific locations and the associated geometrical correlations do produce a significant reduction of $S_{\mathrm{conf}}(E_{\mathrm{fb}})$.

Results reported in this article suggest that strong and fragile liquids are characterized by significant differences in their potential energy landscape properties. A nondegenerate disordered lowest energy state and Gaussian statistics characterize fragile liquids, while a degenerate disordered lowest energy state and logarithmic statistics are associated with strong liquids. These results rationalize the previous landscape analysis of realistic models of network-forming liquids[31] and the recent observation by Saksaengwijit *et al.* that the breakdown of Gaussian landscape statistics is associated with the formation of a connected network.[43] While in atomistic models the lowest energy state is not known and the very long equilibration times prevent an unambiguous determination of its degeneracy, both these quantities are accessible in the present simple model.

A last remark concerns the limit of the $N_{\max}$ value for which the fully connected state can be reached. The possibility of approaching the fully bonded state is limited by the possibility of avoiding the $(T-\phi)$ region where liquid-gas phase separation is present. It has recently been observed[52–54] that the region of unstable states expands on increasing $N_{\max}$ and essentially covers, at low T, the entire accessible ϕ range when $N_{\max} \geqslant 6$. For these large $N_{\max}$ values, slowing down of the dynamics is observed only at very large ϕ, and it is essentially controlled by packing considerations, not by bonding. In this respect, bond-controlled dynamics are observable only when the valence of the interparticle interaction is limited.

ACKNOWLEDGMENTS

We thank K. Binder, A. Heuer, C. De Michele, P. H. Poole, A. M. Puertas, S. Sastry, R. Schilling, N. Wagner, and F. Zamponi for useful discussions and critical readings of the manuscript. MIUR-COFIN and MIUR-FIRB are acknowledged for their financial support. One of the authors (S.V.B.) also acknowledges additional support from NSF. Another author (I.S.V.) acknowledges NSERC-Canada.

[1] P. G. Debenedetti, *Metastable Liquids: Concept and Principles* (Princeton University Press, Princeton, NJ, 1996).
[2] K. Binder and W. Kob, *Glassy Materials and Disordered Solids: An Introduction to their Statistical Mechanics* (World Scientific, Singapore, 2005).
[3] C. A. Angell, J. Non-Cryst. Solids **73**, 1 (1985).
[4] R. Böhmer, K. L. Ngai, C. A. Angell, and D. J. Plazek, J. Chem. Phys. **99**, 4201 (1993).
[5] L. M. Martínez and C. A. Angell, Nature (London) **410**, 663 (2001).
[6] H. Vogel, Z. Phys. **22**, 645 (1921); G. S. Fulcher, J. Am. Ceram. Soc. **8**, 339 (1923); G. Tammann and W. Hesse, Z. Anorg. Allg. Chem. **156**, 245 (1926).
[7] W. Kauzmann, Chem. Rev. (Washington, D.C.) **43**, 219 (1948).
[8] Some polymers of complex architecture display notable differences between T_0, and T_K. See Ref. 9 for a recent discussion on the possible origin of this discrepancy.
[9] D. Cangialosi, A. Alegría, and J. Colmenero, Europhys. Lett. **70**, 614 (2005).
[10] A. Cavagna, I. Giardina, and T. S. Grigera, Europhys. Lett. **61**, 74 (2003); J. Chem. Phys. **118**, 6974 (2003).
[11] F. H. Stillinger, J. Chem. Phys. **88**, 7818 (1988).
[12] J. H. Gibbs and E. A. DiMarzio, J. Chem. Phys. **28**, 373 (1958).
[13] B. Derrida, Phys. Rev. B **24**, 2613 (1981); T. Keyes, J. Chowdhary, and J. Kim, Phys. Rev. E **66**, 051110 (2002); M. Sasai, J. Chem. Phys. **118** 10651 (2003).
[14] T. R. Kirkpatrick and P. G. Wolynes, Phys. Rev. B **36**, 8552 (1987).
[15] M. Mezard and G. Parisi, Phys. Rev. Lett. **82**, 747 (1999).
[16] M. Goldstein, J. Chem. Phys. **51**, 3728 (1969).
[17] F. H. Stillinger and T. A. Weber, Phys. Rev. A **25**, 978 (1982).
[18] F. H. Stillinger and T. A. Weber, Science **225**, 983 (1984); F. H. Stillinger, *ibid.* **267**, 1935 (1995).
[19] D. Wales, *Energy Landscapes* (Cambridge University Press, Cambridge, 2004).
[20] C. A. Angell, Science **267**, 1924 (1995).
[21] F. Sciortino, J. Stat. Mech.: Theory Exp., P05015 (2005).
[22] S. Sastry, P. G. Debenedetti, and F. H. Stillinger, Nature (London) **393**, 554 (1998).
[23] F. Sciortino, W. Kob, and P. Tartaglia, Phys. Rev. Lett. **83**, 3214 (1999).
[24] S. Büchner and A. Heuer, Phys. Rev. E **60**, 6507 (1999).
[25] L. Angelani, R. Di Leonardo, G. Ruocco, A. Scala, and F. Sciortino, Phys. Rev. Lett. **85**, 5356 (2000).
[26] T. S. Grigera, A. Cavagna, I. Giardina, and G. Parisi, Phys. Rev. Lett. **88**, 055502 (2002).
[27] A. Scala, F. W. Starr, E. La Nave, F. Sciortino, and H. E. Stanley, Nature (London) **406**, 166 (2000).
[28] F. Sciortino and P. Tartaglia, Phys. Rev. Lett. **86**, 107 (2001).
[29] S. Sastry, Nature (London) **409**, 164 (2001).
[30] P. G. Debenedetti and F. H. Stillinger, Nature (London) **410**, 259 (2001).
[31] I. Saika-Voivod, P. H. Poole, and F. Sciortino, Nature (London) **412**, 514 (2001); Phys. Rev. E **69**, 041503 (2004).

[32] T. F. Middleton and D. J. Wales, Phys. Rev. B **64**, 024205 (2001).
[33] E. La Nave, A. Scala, F. W. Starr, H. E. Stanley, and F. Sciortino, Phys. Rev. E **64**, 036102 (2001).
[34] F. W. Starr, S. Sastry, E. La Nave, A. Scala, H. E. Stanley, and F. Sciortino, Phys. Rev. E **63**, 041201 (2001).
[35] E. La Nave, S. Mossa, and F. Sciortino, Phys. Rev. Lett. **88**, 225701 (2002).
[36] S. Mossa, E. La Nave, H. E. Stanley, C. Donati, F. Sciortino, and P. Tartaglia, Phys. Rev. E **65**, 041205 (2002).
[37] T. Keyes and J. Chowdhary, Phys. Rev. E **65**, 041106 (2002).
[38] G. Fabricius and D. A. Stariolo, Phys. Rev. E **66**, 031501 (2002).
[39] L. Angelani, G. Ruocco, M. Sampoli, and F. Sciortino, J. Chem. Phys. **119**, 2120 (2003).
[40] B. Doliwa and A. Heuer, Phys. Rev. Lett. **91**, 235501 (2003); Phys. Rev. E **67**, 030501 (2003), **67**, 031506 (2003).
[41] M. Vogel, B. Doliwa, A. Heuer, and S. C. Glotzer, J. Chem. Phys. **120**, 4404 (2004).
[42] R. A. Denny, D. Reichman, and J. P. Bouchaud, Phys. Rev. Lett. **90**, 025503 (2003).
[43] A. Saksaengwijit, J. Reinisch, and A. Heuer, Phys. Rev. Lett. **93**, 235701 (2004).
[44] G. Ruocco, F. Sciortino, F. Zamponi, C. De Michele, and T. Scopigno, J. Chem. Phys. **120**, 10666 (2004).
[45] L. Angelani, G. Foffi, F. Sciortino, and P. Tartaglia, J. Phys.: Condens. Matter **17**, L113 (2005).
[46] A. Attili, P. Gallo, and M. Rovere, Phys. Rev. E **71**, 031204 (2005).
[47] A. Heuer and S. Büchner, J. Phys.: Condens. Matter **12**, 6535 (2000).
[48] A. J. Moreno, S. V. Buldyrev, E. La Nave, I. Saika-Voivod, F. Sciortino, P. Tartaglia, and E. Zaccarelli, Phys. Rev. Lett. **95**, 157802 (2005).
[49] R. J. Speedy and P. G. Debenedetti, Mol. Phys. **81**, 237 (1994); **86**, 1375 (1995); **88**, 1293 (1996).
[50] Y. Duda, C. J. Segura, E. Vakarin, M. F. Holovko, and W. G. Chapman, J. Chem. Phys. **108**, 9168 (1998).
[51] A. Huerta and G. G. Naumis, Phys. Rev. B **66**, 184204 (2002).
[52] E. Zaccarelli, S. V. Buldyrev, E. La Nave, A. J. Moreno, I. Saika-Voivod, F. Sciortino, and P. Tartaglia, Phys. Rev. Lett. **94**, 218301 (2005).
[53] E. Zaccarelli, I. Saika-Voivod, S. V. Buldyrev, A. J. Moreno, P. Tartaglia, and F. Sciortino, J. Chem. Phys. **124**, 124908 (2006).
[54] F. Sciortino, S. V. Buldyrev, C. De Michele *et al.*, Comput. Phys. Commun. **169**, 166 (2005).
[55] D. C. Rapaport, *The Art of Molecular Dynamics Simulation* (Cambridge University Press, Cambridge, UK, 1995).
[56] This approximation for the anharmonic contribution works well in the case of soft potentials as Lennard-Jones 12-6 (Ref. 36), SPC/E water (Ref. 27), or BKS silica (Ref. 31). However, it breaks down in the case of short-range steep potentials (Ref. 45) as that of the model investigated in this work.
[57] D. Frenkel and A. J. C. Ladd, J. Chem. Phys. **81**, 3188 (1984).
[58] D. Frenkel and B. Smit, *Understanding Molecular Simulation* (Academic, San Diego, 1996).
[59] B. Coluzzi, M. Mezard, G. Parisi, and P. Verrocchio, J. Chem. Phys. **111**, 9039 (1999).
[60] N. F. Carnahan and K. E. Starling, J. Chem. Phys. **51**, 635 (1969).
[61] B. J. Alder, D. M. Gass, and T. E. Wainwright, J. Chem. Phys. **53**, 3813 (1970).
[62] J. P. Hansen and I. M. McDonald, *Theory of Simple Liquids* (Academic, New York, 1994).
[63] M. S. Wertheim, J. Stat. Phys. **35**, 19 (1984); **35**, 35 (1984).
[64] R. P. Sear and G. Jackson, J. Chem. Phys. **105**, 1113 (1996).
[65] M. Hemmati, C. T. Moynihan, and C. A. Angell, J. Chem. Phys. **115**, 6663 (2001).
[66] G. Adam and J. H. Gibbs, J. Chem. Phys. **43**, 139 (1965).
[67] J. Kolafa and I. Nezbeda, Mol. Phys. **61**, 161 (1987).
[68] C. Vega and P. A. Monson, J. Chem. Phys. **109**, 9938 (1998).
[69] C. De Michele, S. Gabrielli, F. Sciortino, and P. Tartaglia, cond-mat/0510787.
[70] P. G. Debenedetti, F. H. Stillinger, and M. S. Shell, J. Phys. Chem. B **107**, 14434 (2003).
[71] C. A. Angell and K. J. Rao, J. Chem. Phys. **57**, 440 (1972).
[72] M. G. Sceats, M. Stavola, and S. A. Rice, J. Chem. Phys. **70**, 3927 (1979).
[73] N. Rivier and F. Wooten, MATCH **48**, 145 (2003).
[74] R. J. Speedy, P. G. Debenedetti, R. S. Smith, C. Huang, and B. D. Kay, J. Chem. Phys. **105**, 240 (1996).